

Efficient Implementation of Chemistry in Computational Combustion

Stephen B. Pope · Zhuyin Ren

Received: 20 October 2007 / Accepted: 3 March 2008 / Published online: 2 April 2008
© Springer Science + Business Media B.V. 2008

Abstract For hydrocarbon fuels, detailed chemical kinetics typically involve a large number of chemical species and reactions. In a high-fidelity combustion calculation, it is essential, though challenging, to incorporate sufficiently detailed chemical kinetics to enable reliable predictions of thermo-chemical quantities, especially for pollutants such as NO_x and CO . In this paper, we review the recent work on efficient implementation of chemistry at Cornell, specifically: the invariant constrained equilibrium-edge pre-image curve dimension-reduction method for the reduced description of reactive flows; the transport-chemistry coupling in the reduced description; the computationally efficient operator-splitting schemes for reactive flows; and, recent developments in the storage/retrieval algorithm *in situ* adaptive tabulation.

Keywords Turbulent combustion · Detailed chemistry · Dimension reduction · Operator-splitting · Transport-chemistry coupling · Storage/retrieval

1 Introduction

Today, the numerical simulation of combustion processes plays an important role in the design and analysis of practical combustion devices such as internal combustion engines, industrial burners and furnaces, and gas turbine combustors. Combustion of hydrocarbon fuels is very complicated. A high-fidelity combustion model needs to describe adequately all the physical processes involved such as turbulence and chemical reactions. One of the most challenging tasks is to resolve the highly nonlinear turbulence-chemistry interaction, which requires the accurate descriptions of both

The paper is from the 2nd ECCOMAS Thematic Conference on Computational Combustion.

S. B. Pope (✉) · Z. Ren
Sibley School of Mechanical & Aerospace Engineering,
Cornell University, 254 Upson Hall, Ithaca, NY 14853, USA
e-mail: pope@mae.cornell.edu

the turbulent fluctuations and the combustion chemistry. The straightforward approach to resolve the turbulence-chemistry interaction is direct numerical simulation (DNS) [1, 2], in which the exact governing equations for mass, momentum, energy and all the chemical species are solved. However, the computational requirements of DNS exceed by many orders of magnitude the capacity of present-day computers for virtually all practical turbulent combustion applications. The computational challenges are caused by the large number of unknowns and the wide range of temporal and spatial scales encountered in the governing equations. As a result, numerous turbulent combustion models and efficient algorithms for combustion chemistry have been developed in the past two decades to make the calculation of turbulent combustion feasible without too much loss of accuracy [3–7]. In this article, we focus on discussing the efficient implementation of chemistry in computational combustion.

Detailed/realistic chemical kinetics is essential, though challenging, to be incorporated in computations in order to obtain reliable predictions of thermo-chemical quantities, especially for pollutants such as NO_x , CO and particulates. The computational challenge is due to the large number of chemical species and the wide range of time scales involved in chemical kinetics. Detailed chemistry for hydrocarbon fuels typically involves a large number of chemical species, which participate in tens to thousands of elementary chemical reactions occurring simultaneously within a flow field. In the past decade, substantial advances have been made in our abilities to simulate turbulent combustion. In computations of combustion, hydrocarbon chemistry is being represented in more detail. It is currently feasible to perform calculations of laboratory-scale nonpremixed piloted methane jet flames using the detailed GRI3.0 mechanism which involves 53 species [8–10]. Terascale DNS of three-dimensional, turbulent, temporally-evolving plane CO/H_2 jet flames are reported by Hawkes et al. [11] in which a skeletal $CO + H_2$ mechanism involving 11 species is used. Yet for device-scale combustion processes or combustion of heavier hydrocarbon fuels, the computational cost of directly using detailed chemical kinetics is still large and usually prohibitive. For real and surrogate fuels, chemical mechanisms involving 1000 species or more are not uncommon in the description of the combustion. For example, the detailed mechanism for the primary reference fuels (iso-Octane/*n*-Heptane Mixtures) [12] contains 1034 species which participate in 4326 elementary reactions.

These considerations motivate the well-recognized need for methodologies that radically decrease the computational burden imposed by the direct use of detailed chemical kinetics in reactive flow calculations. Currently, the following approaches are particularly fruitful for the efficient implementation of combustion chemistry:

- Skeletal mechanisms. A skeletal mechanism is extracted from a large detailed mechanism by the elimination of inconsequential species and reactions, such that it is still accurate over a wide range of thermodynamical conditions. The screening for redundant species and reactions can be achieved by methods such as sensitivity analysis [6] and directed relation graphs [13, 14].
- Dimension reduction. This is based on the observation that all compositions which occur in a typical reactive flow lie on (or close to) a low-dimensional manifold in the full composition space. The objective of dimension reduction is to reduce the number of variables required to describe the chemistry accurately. Some existing methods are the quasi-steady state assumption (QSSA) [15, 16],

rate-controlled constrained equilibrium (RCCE) [17, 18], computational singular perturbation [19, 20], intrinsic low-dimensional manifolds (ILDM) [21], trajectory-generated low-dimensional manifolds [22], the Roussel and Fraser algorithm [23], flamelet generated manifolds [24, 25], method of invariant manifolds [26], the approximate slow invariant manifold approach [27], the zero derivative principle method [28], reaction-diffusion manifolds [29], and the invariant constrained equilibrium-edge pre-image curve (ICE-PIC) method [30].

- Storage/retrieval. The objective of storage/retrieval algorithms is to reduce the number of expensive chemistry calculations. Several storage-based methods have been developed in the past such as structured look-up tabulation [31], repro-modelling [32], artificial neural networks (ANN) [33], *in situ* adaptive tabulation (ISAT) [34], and piecewise reusable implementation of solution mapping (PRISM) [35]. Among the existing methods, ISAT is currently particularly fruitful, and it has been widely used to incorporate reduced and detailed chemistry in computations of combustion [8–10, 36–44].
- Adaptive chemistry [45]. Adaptive chemistry is based on the observation that in different regions of a reactive flow field, different chemical species and reactions are dominant. In a limited region of the flow field (correspondingly in a small region in the composition space), the chemical activity can be reproduced accurately by a small subset of the original reactions and species in the detailed mechanism. Instead of solving the flow field with a detailed mechanism appropriate for the full range of conditions that exist within the flow, adaptive chemistry allows the chemistry to ‘adapt’ such that one solves only the minimum required chemistry appropriate for that local area. In other words, the adaptive chemistry approach replaces the detailed mechanism with a number of locally-accurate skeletal mechanisms consisting of a minimum number of species and reactions.

One thing worth mentioning is that the above strategies can be used in combination, and the computational benefits of the combined usage is compounded. For example, the probability density function (PDF) calculation of turbulent methane flames performed in our group [38] have used a 19-species QSSA reduced mechanism, implemented using ISAT. These two measures reduce the computational cost—compared to the direct use of the detailed mechanism—by at least a factor of 1,000, making feasible, in days of computer time, calculations which otherwise would have taken years.

In this paper we review the recent work at Cornell in the areas of dimension reduction (Section 2), coupling reduced chemistry to flow calculations (Section 3), and storage/retrieval algorithms (Section 4). The techniques described are applicable to a general combustion CFD—be it DNS, large-eddy simulation or a PDF method.

2 The ICE-PIC Method of Dimension Reduction

The ICE-PIC method of Ren et al. [30] is developed based on three major ingredients: constrained equilibrium [17, 18]; trajectory-generated manifolds [22]; and, the pre-image curve method [46]. We now provide a brief description of the Invariant Constrained-equilibrium Edge (ICE) manifold, and of the ICE-PIC method. Full details are provided by Ren et al. [30].

To illustrate the methodology, we consider a homogeneous, adiabatic, isobaric, closed system, of fixed enthalpy h and pressure p . Thus the system at time t is fully described by the species specific moles (mass fractions divided by the corresponding species molecular weights), $\mathbf{z}(t) = \{z_1, z_2, \dots, z_{n_s}\}$ of the n_s chemical species. There are n_e elements, and the specific moles of the elements are given by $\mathbf{z}^e = \mathbf{E}^T \mathbf{z}$, where \mathbf{E} is the $n_s \times n_e$ element matrix such that E_{kj} is the number of atoms of element j in a molecule of species k . The system evolves according to the autonomous set of ordinary differential equations

$$\frac{d\mathbf{z}}{dt} = \mathbf{S}(\mathbf{z}(t)), \quad (1)$$

where \mathbf{S} denotes the net rate of change due to chemical reactions. Since elements are conserved, we have $d\mathbf{z}^e/dt = \mathbf{E}^T \mathbf{S} = 0$. We consider \mathbf{z}^e to be known — given by the initial conditions.

In the reduced description, the system is described by n_r reduced composition variables $\mathbf{r}(t) = \{r_1, r_2, \dots, r_{n_r}\}$, which are taken to be the specific moles of the n_e elements \mathbf{z}^e and $(n_r - n_e)$ user-specified variables which can be taken to be the specific moles of $(n_r - n_e)$ user-specified “represented” species. But more generally, linearly-independent combinations of species can be used. In general, the reduced composition \mathbf{r} can be expressed as

$$\mathbf{r} = \mathbf{B}^T \mathbf{z}, \quad (2)$$

where \mathbf{B} is a specified constant $n_s \times n_r$ matrix. For example, if a component of \mathbf{r} is a specified “major” species, then the corresponding column of \mathbf{B} is a unit vector consisting of a single entry (unity) in the row corresponding to the major species.

In the full composition space, realizable values of \mathbf{z} are constrained by the requirements that the specific moles be non-negative ($z_i \geq 0$) and that the specific moles of elements be equal to \mathbf{z}^e (or, equivalently, $\mathbf{E}^T \mathbf{z} = \mathbf{z}^e$). Correspondingly, realizable values of the reduced compositions \mathbf{r} are also confined to the “reduced realizable region”, denoted by \mathcal{B}^+ , which is a convex polytope.

Most dimension-reduction approaches either explicitly or implicitly define (in the n_s -dimensional space of full compositions) an n_r -dimensional manifold, parameterized by the n_r reduced variables \mathbf{r} . Thus there is a function $\mathbf{z}^{\mathcal{M}}(\mathbf{r})$ giving the full compositions on this manifold corresponding to each reduced representation \mathbf{r} in \mathcal{B}^+ . The ICE manifold is defined as follows. For every reduced composition \mathbf{r} on the boundary $\partial\mathcal{B}^+$ of \mathcal{B}^+ , $\mathbf{z}^{ICE}(\mathbf{r})$ is defined to be the constrained equilibrium composition $\mathbf{z}^{CE}(\mathbf{r})$. That is, of all compositions \mathbf{z} satisfying $\mathbf{B}^T \mathbf{z} = \mathbf{r}$ (for the given \mathbf{r} in $\partial\mathcal{B}^+$), $\mathbf{z}^{CE}(\mathbf{r})$ is the unique composition of maximum entropy. This defines the constrained-equilibrium edge of the ICE manifold. The interior of the ICE manifold is then generated simply by following the reaction trajectories (i.e., solutions to Eq. 1) from every point on the constrained-equilibrium edge. Thus, by construction, being composed of reaction trajectories, the ICE manifold is invariant. Moreover the ICE manifold is continuous and piecewise smooth. With a reasonable choice of represented species (e.g., including major reactants, products, and important radicals), the manifold is not folded, and hence is given by a graph of a function of the reduced variables, i.e., $\mathbf{z}^{ICE}(\mathbf{r})$. In other words, there is a unique ICE manifold point \mathbf{z}^{ICE} corresponding to every value of \mathbf{r} in \mathcal{B}^+ . At the current stage, the dimensionality n_r of the ICE manifold is specified manually. Then accuracy tests can be performed

to determine whether or not the specified dimensionality is suitable for particular reactive flows.

The above description implicitly yields a method by which the whole ICE manifold can be generated. However, to implement dimension-reduction strategies efficiently, it is necessary to have a local means of “species reconstruction”, that is, a method of determining $\mathbf{z}^M(\mathbf{r})$ for a specified value of \mathbf{r} . As described in Ren et al. [30], the ICE-PIC method achieves this local species reconstruction based on the constrained-equilibrium pre-image curve. In comparison to other existing methods such as QSSA, RCCE and ILDM, this method is the first approach that locally determines compositions on a low-dimensional invariant manifold. Because it is local, the ICE-PIC method can readily be applied to high-dimensional systems.

From the species reconstruction perspective, the accuracy of the ICE-PIC method has been examined in autoignition and in one-dimensional laminar flames of hydrogen/air and methane/air mixtures [30, 47]. Those studies demonstrate that the local errors incurred by ICE-PIC, i.e., the errors in the reconstructed composition or the rate-of-change vector, are well controlled. For example, Fig. 1 shows the normalized errors in the reconstructed composition and the rate-of-change for three different methods. It is readily observed that the ICE-PIC method yields errors typically 2 or 3 orders of magnitude smaller than those incurred by the corresponding RCCE method. With 7 degrees of freedom, the ICE-PIC method yields comparably accurate results with ARM1, which has 12 degree of freedom. Those studies also demonstrate that while the existence of the reconstructed composition is guaranteed by RCCE and ICE-PIC, there is no such guarantee with ILDM. The ILDM may not exist in low-temperature region.

The capability of the ICE-PIC method for the reduced description of reactive flows is recently demonstrated in the calculations of the oxidation of CO and H_2 in a continuously stirred tank reactor (CSTR) [48]. The system exhibits complex dynamics such as oscillatory ignition, which are particularly challenging for the reduced description by dimension-reduction methods. In the reduced description, a set of governing equations for the reduced compositions is solved, with the ICE-PIC method being used to perform species reconstruction and to evaluate the rate-of-

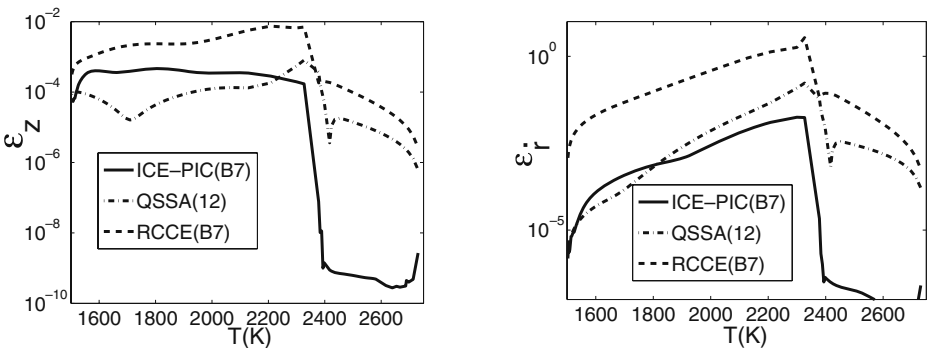


Fig. 1 Normalized species reconstruction errors as functions of temperature for the autoignition of stoichiometric CH_4/air at 1 atm. QSSA(12) denotes the ARM1 QSSA method in which there are 12 degrees of freedom; ICE-PIC and RCCE have the same reduced representation with 7 degrees of freedom. The detailed mechanism involves 31 species, i.e., 31 degrees of freedom

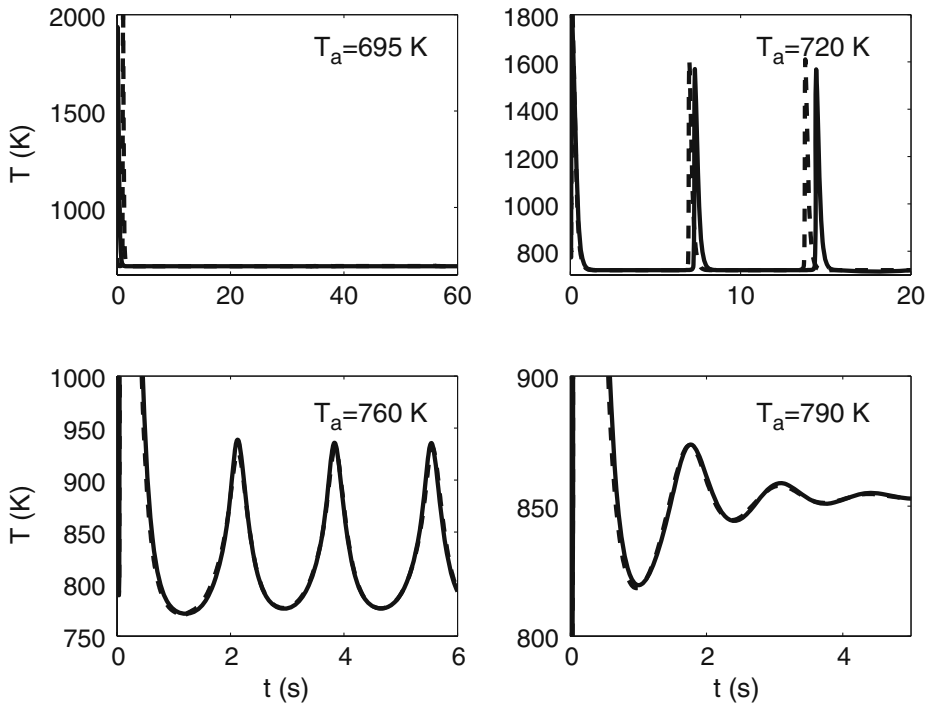


Fig. 2 Comparison at different ambient temperatures T_a with $P = 25$ Torr between the full description (*solid lines*) and the reduced description (*dashed lines*) of the complex dynamics exhibited by the reaction of a $CO/H_2/O_2$ mixture in an isobaric CSTR. The full description incorporates the full set of 11 chemical species. The reduced description is provided by the ICE-PIC method with H_2 , O_2 , CO , H , and O being the represented species

change of the reduced compositions whenever necessary. It is shown that the reduced description provided by the ICE-PIC method (with 5 degrees of freedom) is capable of quantitatively reproducing the complex dynamics exhibited in a CSTR (described by an 11-species detailed mechanism). Figure 2 shows the predicted temperature profiles by the ICE-PIC method with five represented species at different ambient temperatures T_a . As may be seen from the figure, the reduced description successfully reproduces the dynamics in the regions of steady slow reaction, oscillatory ignition, and steady ignited state.

3 The Use of Reduced Chemistry in Computations of Reacting Flows

3.1 Splitting schemes

Much of the computational cost in combustion calculations with detailed or reduced chemistry is associated with the evaluation of chemistry. One effective computational approach to alleviate the problem of large demands on computational time on chemistry evaluation is operator splitting, wherein the portions of the governing equations containing chemical reaction terms are separated from other parts such as transport

terms. For the reaction sub-steps, efficient solutions can be obtained by using the storage/retrieval method ISAT [34] by taking advantage of unique characteristics of the underlying system of equations. ISAT has been used beneficially in conjunction with operator-splitting schemes. All of the PDF calculations from the Cornell group (e.g., [8, 9, 36–38]) used operator-splitting in the context of PDF calculations of turbulent reacting flows. The calculations showed that an operator-split formulation coupled with ISAT can speed-up PDF calculations by a factor of 100–1000 over the use of direct evaluation of chemistry.

Recently operator-splitting schemes combined with ISAT for unsteady reactive flow calculations with detailed chemistry are developed by Singer and Pope [41, 42]. The application of ISAT to unsteady reactive flows (e.g., unsteady laminar flames) is challenging because of the strong coupling between reaction and diffusion and because of the evolving flow. The splitting schemes are based on the Strang splitting technique [49] wherein the chemical reactions are separated from convection and diffusion. As demonstrated, the schemes achieve second-order accuracy in space through the use of centered-finite differences; second-order accuracy in time is achieved through Strang splitting. The reaction sub-steps are computed using ISAT. The schemes have been applied to both one- and two-dimensional premixed laminar flames. As demonstrated, when the ISAT-based splitting scheme is applied to a one-dimensional methane-air flame using detailed chemical kinetics (i.e., GRI3.0), an overall speed-up factor of approximately 7.5 is achieved after the ISAT table has been constructed and populated.

In the reduced description of a reacting flow, the system is described in terms of n_r reduced composition variables \mathbf{r} for which the evolution equations can be in general written as

$$\frac{\partial \mathbf{r}}{\partial t} = \mathbf{S}_r(\mathbf{r}, \mathbf{w}(\mathbf{r})) + \mathbf{M}(\mathbf{r}, \mathbf{w}(\mathbf{r})), \quad (3)$$

where: \mathbf{S}_r (of dimension n_r) denotes the rate-of-change of the reduced variables due to chemical reactions; and \mathbf{M} (of dimension n_r) denotes the rate-of-change of the reduced variables due to transport processes such as convection and molecular diffusion. The variables \mathbf{w} (of dimension n_w), which are known functions of \mathbf{r} , are called secondary variables, which are the concentrations of unrepresented species or other derived quantities. As indicated in Eq. 3, in the reduced description, the secondary variables \mathbf{w} , which are functions of \mathbf{r} , are needed for evaluating the reaction term and transport term in the governing equations. In the reduced description provided by different dimension-reduction methods such as the QSSA method [15], the RCCE method [17], and the ICE-PIC method [47], the evaluation of $\mathbf{w}(\mathbf{r})$ is computationally expensive.

In [50], Ren and Pope developed computationally-efficient splitting schemes for solving the above class of reaction-transport problems. The schemes separate chemical reaction terms from transport terms. Two classes of splitting schemes are introduced: one is based on the Strang splitting technique, and the other is based on staggered time steps. For each time step Δt , schemes based on Strang splitting require two reaction sub-steps of length $\Delta t/2$ and one transport sub-step of length Δt . Schemes based on staggered time steps require a single reaction fractional step of length Δt and a single transport sub-step of length Δt . For the reaction sub-steps, efficient solutions can be obtained using ISAT. The computationally efficient solution to the transport sub-step is achieved through predictor-corrector methods

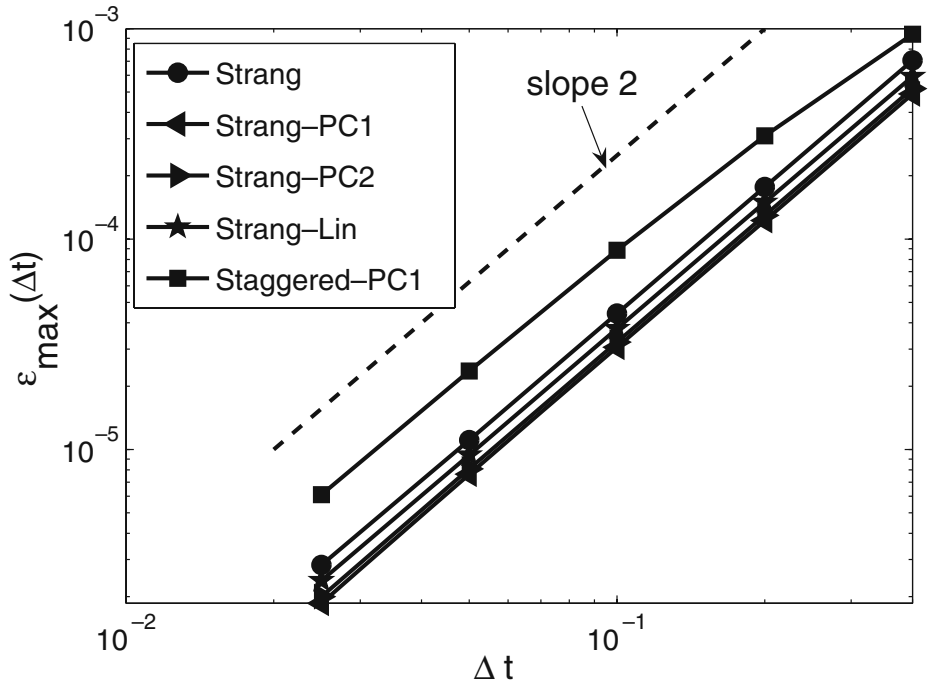


Fig. 3 Demonstration of the accuracy of different splitting schemes for the reduced description of the extended Davis-Skodjie model system [51, 52]. The governing equations are $dr_1/dt = -r_1u \exp(-r_2) + (r_1^{in} - r_1)/t_{res}$ and $dr_2/dt = 0 + (r_2^{in} - r_2)/t_{res} + r_1u^2$, with $\mathbf{r} \equiv [r_1; r_2]$ being the primary variables, u (a function of \mathbf{r}) being the secondary variable, t_{res} being the specified residence time, and \mathbf{r}^{in} being the specified inflow condition. The first terms on the right-hand side of the equations represent reaction and the second terms on the right-hand side represent transport (i.e., inflow/outflow). This model is an abstraction of the reduced description of the Davis-Skodjie reactive model in a CSTR. In this model, r_1 and u correspond to chemical species, and r_2 corresponds to temperature. The secondary variable u is related to the primary variables through the function $u = r_1/(1 + r_1)$, which is assumed to be computationally expensive to evaluate for the purpose of demonstration of different splitting schemes in a simple model problem. The residence time is taken to be $t_{res} = 2$, the inflow conditions are $\mathbf{r}^{in} = [1; 1]$, and the initial conditions are $\mathbf{r} = [1; 1]$. Figure shows the numerical errors of the Strang scheme, modified Strang schemes (Strang-PC1, Strang-PC2, Strang-Lin) and a Staggered scheme (Staggered-PC1) against the time step. Also shown is the dashed line of slope 2 corresponding to second-order accuracy ($\epsilon_{max}(\Delta t) \sim \Delta t^2$)

or linearization. As demonstrated in the test problems, the proposed splitting schemes, which yield the efficient solution to transport sub-step, achieve second-order accuracy. For example, Fig. 3 shows the numerical errors of the proposed splitting schemes against the time step when applied for the reduced description of the extended Davis-Skodjie model system [51, 52]. As shown in the plot, for the proposed splitting schemes, over a wide range of Δt , the error decreases with Δt , essentially as Δt^2 , thus illustrating their second-order accuracy in time.

3.2 Transport-chemistry coupling

Most of the existing dimension reduction methods, such as QSSA, ILDM, RCCE and ICE-PIC, are developed based on spatially homogeneous systems absent of

transport processes such as convection and molecular diffusion. The corresponding low-dimensional manifold, referred to as “chemistry-based”, is identified solely based on chemical kinetics. The use of these chemistry-based manifolds to describe inhomogeneous reactive flows is complicated by the transport processes present and the resulting transport-chemistry coupling.

For general combustion processes, chemical kinetics have a much wider range of time scales than those of transport processes. Previous studies [52–58] show that due to the fast chemical time scales, the compositions are not exactly on, but are close to chemistry-based slow manifolds. The full compositions can be expressed as

$$\mathbf{z}(\mathbf{x}, t) = \mathbf{z}^{\mathcal{M}}(\mathbf{r}(\mathbf{x}, t)) + \delta\mathbf{z}(\mathbf{x}, t), \tag{4}$$

where $\delta\mathbf{z}(\mathbf{x}, t)$ is the departure from the manifold, which is defined to be in the unrepresented subspace, i.e.,

$$\delta\mathbf{z} = \mathbf{U}\delta\mathbf{u}, \tag{5}$$

with \mathbf{U} being a constant $n_s \times n_u$ matrix with orthonormal columns spanning the unrepresented subspace and

$$\delta\mathbf{u} = \mathbf{U}^T [\mathbf{z}(\mathbf{x}, t) - \mathbf{z}^{\mathcal{M}}(\mathbf{r}(\mathbf{x}, t))]. \tag{6}$$

The following factors may cause the compositions to depart from the manifold: the manifold not being invariant; the transport processes such as molecular diffusion; and, initial and boundary compositions not lying on the manifold. Even if the composition perturbations off the chemistry-based manifold are “small”, these seemingly “small” perturbations introduce three terms in the governing equations for the reduced compositions, which in general are of leading order. The effect of initial and boundary conditions on the reduced description has been studied in Ref. [58]. In this paper, we provide an overview the “close-parallel” approach of Ren et al. [47] to quantify the non-invariance effect and the transport effect on the compositions and the reduced description. Full details are provided in [47, 52, 59].

To demonstrate the coupling between reduced chemistry and transport, we consider an inhomogeneous reactive flow, where the pressure p and enthalpy h are taken to be constant and uniform (although the extension to variable pressure and enthalpy is straightforward). The system at time t is then fully described by the full composition $\mathbf{z}(\mathbf{x}, t)$, which varies both in space, \mathbf{x} , and time, t . The full composition \mathbf{z} is taken to be the specific species moles. The system evolves according to the set of n_s PDEs

$$\frac{\partial}{\partial t}\mathbf{z}(\mathbf{x}, t) + v_i \frac{\partial \mathbf{z}}{\partial x_i} = \mathbf{D}\{\mathbf{z}(\mathbf{x}, t)\} + \mathbf{S}\{\mathbf{z}(\mathbf{x}, t)\}, \tag{7}$$

where \mathbf{S} denotes the rate-of-change of the full composition due to chemical reactions. The spatial transport includes the convective contribution ($v_i \partial \mathbf{z} / \partial x_i$, where $\mathbf{v}(\mathbf{x}, t)$ is the velocity field) and the diffusive contribution (\mathbf{D}). In calculations of reactive flows, one simplified model widely used for diffusion is

$$\mathbf{D}\{\mathbf{z}\} = \frac{1}{\rho} \nabla \cdot (\rho \mathbf{\Gamma} \nabla \mathbf{z}), \tag{8}$$

where ρ is the mixture density, and $\mathbf{\Gamma}$ is a diagonal matrix with the diagonal components $\Gamma_1, \Gamma_2, \dots, \Gamma_{n_s}$ being the mixture-averaged species diffusivities, which are usually functions of \mathbf{z} .

In the reduced description, the reactive system is described in terms of a smaller number n_r of reduced composition variables \mathbf{r} . The exact evolution equation for $\mathbf{r}(\mathbf{x}, t)$ is obtained by pre-multiplying Eq. 7 with the matrix \mathbf{B}^T to yield

$$\frac{\partial \mathbf{r}}{\partial t} + v_i \frac{\partial \mathbf{r}}{\partial x_i} = \mathbf{B}^T \mathbf{D}\{\mathbf{z}\} + \mathbf{B}^T \mathbf{S}(\mathbf{z}). \tag{9}$$

In the reduced description, the task is to express the right-hand side of Eq. 9 ($\mathbf{B}^T \mathbf{D}\{\mathbf{z}\} + \mathbf{B}^T \mathbf{S}(\mathbf{z})$) as a function of \mathbf{r} . The most straightforward approach, denoted as the “first approximation” in Ref. [47], is to completely neglect the departures $\delta \mathbf{z}$ and assume that the compositions in the reactive flow lie on the chemistry-based manifold, i.e.,

$$\mathbf{z}(\mathbf{x}, t) = \mathbf{z}^{\mathcal{M}}(\mathbf{r}(\mathbf{x}, t)). \tag{10}$$

Hence the evolution equation for the reduced composition variables according to the “first approximation” is

$$\frac{\partial \mathbf{r}}{\partial t} + v_i \frac{\partial \mathbf{r}}{\partial x_i} = \mathbf{B}^T \mathbf{D}\{\mathbf{z}^{\mathcal{M}}(\mathbf{r})\} + \mathbf{B}^T \mathbf{S}(\mathbf{z}^{\mathcal{M}}(\mathbf{r})). \tag{11}$$

As shown in Fig. 4, even for a simple model problem, by neglecting the transport effect in the reduced description, “first approximation” gives a qualitatively inaccurate evolution of the reduced composition compared with the full model

In the “close-parallel” approach, the compositions are assumed to lie on a low-dimensional manifold which is close to and parallel to the chemistry-based manifold. In other word, in the inhomogeneous flow, the full system evolves on a manifold which is close to and parallel to the chemistry-based manifold employed. By

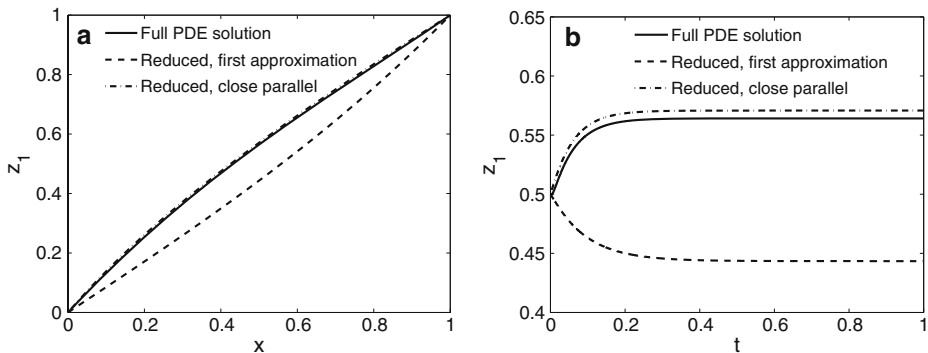


Fig. 4 Full description and reduced description of the two-variable model system $\partial z_1 / \partial t = 1/\varepsilon(z_2 - z_1) - z_1 + \nabla \cdot (D_1 \nabla z_1)$ and $\partial z_2 / \partial t = -1/\varepsilon(z_2 - z_1) - z_1 + \nabla \cdot (D_2 \nabla z_2)$ with $\varepsilon = 0.01$, $D_1 = 1$ and $D_2 = D_1 + 3x$. Based on the reaction source term, the 1-dimensional attracting manifold is $\mathbf{z} = [z_1; z_2] = \mathbf{z}^{\mathcal{M}}(z_1) = [z_1; z_1]$. The length of the physical domain is set to be $L = 1$. The boundary conditions are on the manifold and given by $[z_1(t, x = 0); z_2(t, x = 0)] = [0; 0]$ and $[z_1(t, x = 1); z_2(t, x = 1)] = [1; 1]$. Initially, $z_1(t = 0, x)$ is linear in x , and $z_2(t = 0, x)$ is determined so that the full compositions are initially on the attracting manifold. In the reduced representation, z_1 is the represented variable. **a**: distribution of z_1 at $t = 1$; **b**: evolution of z_1 at $x = \frac{1}{2}$

substituting $\mathbf{z}(\mathbf{x}, t) = \mathbf{z}^{\mathcal{M}}(\mathbf{r}(\mathbf{x}, t)) + \delta\mathbf{z}(\mathbf{x}, t)$ and $\delta\mathbf{z} = \mathbf{U}\delta\mathbf{u}$ into Eq. 9, with the “close-parallel” assumption, we obtain

$$\frac{\partial \mathbf{r}}{\partial t} + v_i \frac{\partial \mathbf{r}}{\partial x_i} = \mathbf{B}^T \mathbf{D}\{\mathbf{z}^{\mathcal{M}}(\mathbf{r})\} + \mathbf{B}^T \mathbf{S}(\mathbf{z}^{\mathcal{M}}(\mathbf{r})) + \mathbf{B}^T \mathbf{J}\mathbf{U}\delta\mathbf{u}, \tag{12}$$

where $J_{ij} \equiv \partial S_i / \partial z_j |_{\mathbf{z}=\mathbf{z}^{\mathcal{M}}}$ is the Jacobian matrix. The last term in Eq. 12 is not negligible because small perturbations off the manifold may result in significant changes in the reaction rate due to fast processes in the chemical kinetics. As shown in Refs. [47, 52], with the close-parallel assumption, by considering the balance equation in the normal subspace of the manifold, the perturbation $\delta\mathbf{z}$ ($=\mathbf{U}\delta\mathbf{u}$) is obtained as

$$\delta\mathbf{u} = -(\mathbf{N}^T \mathbf{J}(\mathbf{z}^{\mathcal{M}}) \mathbf{U})^{-1} [\mathbf{N}^T \mathbf{D}\{\mathbf{z}^{\mathcal{M}}\} + \mathbf{N}^T \mathbf{S}(\mathbf{z}^{\mathcal{M}})], \tag{13}$$

where \mathbf{N} is an $n_s \times (n_s - n_r)$ matrix with orthonormal columns spanning the normal subspace. As may be seen from Eq. 13, the compositions in the inhomogeneous reactive flows are pulled off the slow manifold due to the molecular diffusion and the non-invariance of the manifold.

Substituting Eq. 13 into Eq. 12, we have the evolution equations for the reduced composition variable \mathbf{r}

$$\frac{\partial \mathbf{r}}{\partial t} + v_i \frac{\partial \mathbf{r}}{\partial x_i} = \mathbf{B}^T \mathbf{D}\{\mathbf{z}^{\mathcal{M}}(\mathbf{r})\} + \mathbf{B}^T \mathbf{S}(\mathbf{z}^{\mathcal{M}}(\mathbf{r})) + \mathbf{H}^T \mathbf{S}(\mathbf{z}^{\mathcal{M}}) + \mathbf{H}^T \mathbf{D}\{\mathbf{z}^{\mathcal{M}}\} \tag{14}$$

where $\mathbf{H}^T \equiv -\mathbf{B}^T \mathbf{J}\mathbf{U}(\mathbf{N}^T \mathbf{J}\mathbf{U})^{-1} \mathbf{N}^T$ is an $n_r \times n_s$ matrix. Compared to the “first approximation” (Eq. 11), there are two extra terms that arise, respectively, from the non-invariance effect and transport-chemistry coupling. If the manifold is invariant, then \mathbf{S} lies in the tangent subspace, and hence $\mathbf{N}^T \mathbf{S}$ is zero, and so $\mathbf{H}^T \mathbf{S}$ is also zero. Thus, as indicated by its name, the “non-invariance effect” $\mathbf{H}^T \mathbf{S}$ arises (for non-invariant manifolds) from \mathbf{S} not being exactly in the tangent subspace (i.e., from $\mathbf{N}^T \mathbf{S}$ being non-zero).

Equation 14 can be explored further to show explicitly the dissipation-curvature effect and differential diffusion effect on the reduced description of reactive flows. We consider the decomposition of the diagonal diffusivity matrix Γ as

$$\Gamma = \bar{\Gamma} \mathbf{I} + \delta\Gamma, \tag{15}$$

where $\bar{\Gamma}$ is a reference diffusivity, chosen to make $\delta\Gamma$ small in some sense. A natural choice of $\bar{\Gamma}$ is the species-weighted diffusivity $\|\Gamma \mathbf{z}^{\mathcal{M}}\| / \|\mathbf{z}^{\mathcal{M}}\|$. Substituting Eqs. 8 and 15 into 14, we obtain (after some manipulation)

$$\begin{aligned} \frac{\partial \mathbf{r}}{\partial t} + v_i \frac{\partial \mathbf{r}}{\partial x_i} = & \mathbf{B}^T \mathbf{D}\{\mathbf{z}^{\mathcal{M}}(\mathbf{r})\} + \mathbf{B}^T \mathbf{S}(\mathbf{z}^{\mathcal{M}}(\mathbf{r})) \\ & + \mathbf{H}^T \mathbf{S}(\mathbf{z}^{\mathcal{M}}) + \mathbf{H}^T \frac{\partial^2 \mathbf{z}^{\mathcal{M}}}{\partial r_j \partial r_k} \left(\bar{\Gamma} \frac{\partial r_j}{\partial x_i} \frac{\partial r_k}{\partial x_i} \right) + \mathbf{H}^T \frac{1}{\rho} \nabla \cdot (\rho \delta\Gamma \nabla \mathbf{z}^{\mathcal{M}}), \end{aligned} \tag{16}$$

where \mathbf{H} provides the coupling information between the reduced composition and chemistry. Hence in general reactive flows, the transport processes introduce two usually non-trivial coupling terms in the reduced composition evolution equation: one is due to the combination of scalar dissipation and manifold curvature, the other

is due to differential diffusion. These two terms represent the transport-chemistry coupling.

In short, in an inhomogeneous reactive flow, three different mechanisms pull compositions off the chemistry-based slow manifold: “non-invariance”, “dissipation-curvature” and “differential diffusion”. Correspondingly, these three perturbations introduce three usually non-trivial terms in the evolution equation of the reduced composition variables. Hence the “first approximation”, which simply neglects these “small” perturbations (and therefore neglects the usually non-trivial terms in the evolution equation of the reduced composition variable) is in general inaccurate. In general, in the reduced description, the transport-chemistry coupling has to be appropriately accounted for by using an approach such as the “close-parallel” approach. As shown in Fig. 4, by incorporating the transport-chemistry coupling in this way, the accuracy of the reduced description can be substantially improved.

4 Storage/Retrieval Algorithms

All of the PDF calculations from the Cornell group (e.g., [9]) use *in situ* adaptive tabulation [34] to implement the combustion chemistry. ISAT is also used in the transported PDF method implemented in Fluent which has been used by Gordon et al. [43, 44] among others.

Since its original development in the mid 1990s, the ISAT algorithm has been improved in terms of accuracy, efficiency and parallel implementation [39, 40]. Here we describe the improvement brought about by the incorporation of *error checking and correction* (ECC), which is an idea due to Panda (private communication).

Briefly stated, ISAT is used to tabulate a function $\mathbf{f}(\mathbf{x})$, where \mathbf{f} and \mathbf{x} are vectors of length n_f and n_x respectively. In its simplest implementation in PDF methods, \mathbf{x} is the composition of a particle prior to the reaction sub-step, and \mathbf{f} is the composition after the sub-step. Thus n_x and n_f are both of order the number of species. On the q -th “query”, given $\mathbf{x}^{(q)}$, ISAT returns $\mathbf{f}^{(q)}$ which is an approximation to $\mathbf{f}(\mathbf{x}^{(q)})$. There is a tabulation error involved $\varepsilon^{(q)} = |\mathbf{f}^{(q)} - \mathbf{f}(\mathbf{x}^{(q)})|$ which is controlled by a specified error tolerance ε_{tol} . The error incurred on the many queries has a distribution, which is characterized by the 90th percentile error, $\varepsilon_{0.9}$. Thus, by definition for 90% of the queries, $\varepsilon^{(q)}$ is less than $\varepsilon_{0.9}$. For a given implementation of ISAT and for a given test case, $\varepsilon_{0.9}$ varies (almost) linearly with ε_{tol} : but the ratio $\varepsilon_{0.9}/\varepsilon_{tol}$ can be affected by the particulars of the implementation.

The ECC augmentation to the ISAT algorithm produces a significant decrease in $\varepsilon_{0.9}/\varepsilon_{tol}$ at a modest computational cost. On randomly selected queries, q , the exact value $\mathbf{f}(\mathbf{x}^{(q)})$ is evaluated (in addition to obtaining the approximate value $\mathbf{f}^{(q)}$ from ISAT) so that the error $\varepsilon^{(q)}$ can be measured. This is an expensive process, and the frequency of performing these operations is controlled so that the CPU time consumed is a specified fraction ζ of the total. If $\varepsilon^{(q)}$ is less than ε_{tol} , the query is deemed to be accurate and no further action is taken. But if $\varepsilon^{(q)}$ exceeds ε_{tol} , the “ellipsoid of accuracy” (EOA) used to obtain $\mathbf{f}^{(q)}$ is shrunk to include $\mathbf{x}^{(q)}$. (See Pope [34] for an explanation of EOA, and related concepts.) This process not only eliminates the error on the query in question, but it prevents (or at least decreases the chances of) inaccurate approximations on subsequent queries with similar values of $\mathbf{x}^{(q)}$.

Fig. 5 CPU time (μs) per query against 90% error for partially stirred tank reactor test of ISAT with ECC. Error tolerance $\varepsilon_{tol} = 1 \times 10^{-4}$ (green), 2×10^{-4} (blue), 3×10^{-4} (red); the numbers 0, 0.01, 0.03, 0.1, 0.3, 0.5 indicate the value of ζ controlling the amount of ECC performed

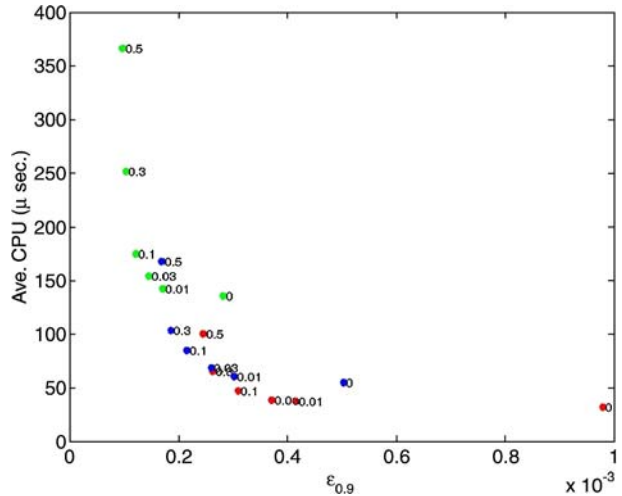


Figure 5 shows results demonstrating the performance of ISAT with ECC. The results come from a partially stirred tank reactor test case of non-premixed combustion, using a 16-species skeletal mechanism, 100 particles, 10^6 time steps, resulting in 10^8 queries. There are 18 separate tests corresponding to all combinations of $\varepsilon_{tol} = 1 \times 10^{-4}$, 2×10^{-4} , 3×10^{-4} and $\zeta = 0, 0.01, 0.03, 0.1, 0.3, 0.5$. For $\varepsilon = 3 \times 10^{-4}$ and $\zeta = 0$, the incurred error $\varepsilon_{0.9}$ is a little less than 10^{-3} . Increasing ζ from 0 to 0.01 results in more than halving $\varepsilon_{0.9}$ with a negligible CPU penalty. As ζ is increased, $\varepsilon_{0.9}$ decreases, but the CPU time increases. The optimal value of ζ is around 0.1. With this value, the CPU time required to achieve a given value of $\varepsilon_{0.9}$ is about halved (compared to using $\zeta = 0$).

In addition to demonstrating the effectiveness of ECC, these results highlight the fact that comparison of the computational performance of different tabulation methodologies must take account of the level of tabulation error incurred. Performance is best compared for a fixed level of tabulation error.

5 Conclusions

In a large-scale calculation of combustion processes burning complex hydrocarbon fuels, efficient implementation of chemistry is a necessity to make the computation affordable. In this paper we review the recent work at Cornell in the areas of dimension reduction, coupling reduced chemistry to flow calculations, and storage/retrieval algorithms.

The recently developed ICE-PIC dimension-reduction method [30] for the reduced description of reactive flows is based on three major ingredients: constrained equilibrium; trajectory-generated manifolds; and, the pre-image curve method. The low-dimensional manifold identified, the ICE manifold, is invariant, continuous and piecewise smooth. With a reasonable choice of represented species, the manifold is not folded. The ICE-PIC method achieves local species reconstruction based on the constrained-equilibrium pre-image curve. Hence it can readily be applied to high-

dimensional systems. In comparison to other existing methods such as QSSA, RCCE and ILDM, this method is the first approach that locally determines compositions on a low-dimensional invariant manifold.

The accuracy of the ICE-PIC method has been examined in autoignition and in one-dimensional laminar flames of hydrogen/air and methane/air mixtures [30, 47]. Those studies demonstrate that the local errors incurred by ICE-PIC (e.g., the errors in the reconstructed composition) are well controlled. The capability of the ICE-PIC method for the reduced description of reactive flows is demonstrated through the calculation of the oxidation of CO/H_2 in a CSTR. It is shown that the reduced description provided by the ICE-PIC method is capable of quantitatively reproducing the complex dynamics.

One effective computational approach to alleviate the computational time on chemistry evaluation is operator splitting wherein chemical reaction is separated from transport processes. By doing so, for the reaction sub-steps, efficient solutions can be obtained by using ISAT. Recently operator-splitting schemes combined with ISAT for unsteady reactive flow calculations with detailed chemistry are developed by Singer and Pope [41, 42]. The scheme achieves second-order accuracy in space through the use of centered-finite differences; and second-order accuracy in time is achieved through Strang splitting. The schemes have been applied to both one- and two-dimensional premixed laminar flames.

In [50], Ren and Pope developed computationally efficient splitting schemes for the reduced description of reacting flows. Two classes of splitting schemes are introduced: one is based on the Strang splitting technique, and the other is based on staggered time steps. For each time step Δt , schemes based on Strang splitting require two reaction sub-steps of length $\Delta t/2$ and one transport sub-step of length Δt . Schemes based on staggered time steps require a single reaction fractional step of length Δt and a single transport sub-step of length Δt . For the reaction sub-steps, efficient solutions can be obtained using ISAT. The computationally-efficient solution of the transport sub-step is achieved through predictor-corrector methods or linearization. As demonstrated in the test problems, the splitting schemes, which yield efficient solutions to the transport sub-step, achieve second-order accuracy.

The use of chemistry-based manifolds to describe inhomogeneous reactive flows is complicated by the transport processes present. Three different mechanisms “non-invariance”, “dissipation-curvature” and “differential diffusion” pull compositions off the chemistry-based manifold. The corresponding perturbations introduce three usually non-trivial terms, referred to as transport-chemistry coupling, in the evolution equation of the reduced composition variables. The “first approximation”, which simply neglects the perturbations and therefore neglects the transport-chemistry coupling in the evolution equation of the reduced composition variables, is in general inaccurate. It is shown that the transport-chemistry coupling can be accurately accounted for by the “close-parallel” approach, which assumes that the compositions lie on a low-dimensional manifold which is close to and parallel to the chemistry-based slow manifold.

The storage/retrieval algorithm ISAT has been widely used to incorporate the reduced/detailed chemical mechanism in the calculation of turbulent combustion. In this paper, the ECC augmentation to the ISAT algorithm is discussed. It is shown that the ECC augmentation produces a significant decrease in the incurred tabulation error at a modest computational cost. Using the optimal amount of ECC, the CPU

time required to achieve a given level of accuracy is about halved (compared to not using ECC).

The ongoing work includes a computationally-efficient implementation of ICE-PIC with ISAT for application to the simulation and modelling of turbulent combustion.

Acknowledgement This research is supported by the National Science Foundation through Grant No. CBET-0426787.

References

1. Poinso, T., Veynante, D.: Theoretical and Numerical Combustion, 1st edn. R.T. Edwards Inc., Philadelphia (2001)
2. Pope, S.B.: Turbulent Flows. Cambridge University Press, Cambridge (2000)
3. Bilger, R.W., Pope, S.B., Bray, K.N.C., Driscoll, J.F.: Paradigms in turbulent combustion research. Proc. Combust. Inst. **30**, 21–42 (2005)
4. Law, C.K.: Combustion Physics. Cambridge University Press, Cambridge (2006)
5. Peters, N.: Turbulent Combustion. Cambridge University Press, Cambridge (2000)
6. Tomlin, A.S., Turányi, T., Pilling, M.J.: Mathematical Tools for the Construction, Investigation and Reduction of Combustion Mechanisms. Comprehensive Chemical Kinetics 35: Low-temperature Combustion and Autoignition. Elsevier, Amsterdam (1997)
7. Warnatz, J., Maas, U., Dibble, R.W.: Combustion: Physical and Chemical Fundamentals, Modeling and Simulation, Experiments, Pollutant Formation, 3rd edn. Springer, Berlin Heidelberg New York (2001)
8. Cao, R., Pope, S.B.: The influence of chemical mechanisms on PDF calculations of nonpremixed piloted jet flames. Combust. Flame **143**, 450–470 (2005)
9. Cao, R., Wang, H., Pope, S.B.: The effect of mixing models in PDF calculations of piloted jet flames. Proc. Combust. Inst. **31**, 1543–1550 (2007)
10. Wang, H., Pope, S.B.: Comparison of detailed reaction mechanisms in non-premixed combustion. Combust. Flame (2008, submitted)
11. Hawkes, E.R., Sankaran, R., Sutherland, J.C., Chen, J.H.: Scalar mixing in direct numerical simulations of temporally evolving plane jet flames with skeletal CO/H_2 kinetics. Proc. Combust. Inst. **31**, 1633–1640 (2007)
12. Curran, H.J., Gaffuri, P., Pitz, W.J., Westbrook, C.K.: A comprehensive modeling study of iso-octane oxidation. Combust. Flame **129**, 253–280 (2002)
13. Lu, T., Law, C.K.: A directed relation graph method for mechanism reduction. Proc. Combust. Inst. **30**, 1333–1341 (2005)
14. Pepiot, P., Pitsch, H.: Systematic reduction of large chemical mechanisms. Paper presented at the 4th joint meeting of the U. S. Sections of the Combustion Institute, Philadelphia, PA, 21–23 March 2005
15. Bodenstein, M., Lind, S.C.: Geschwindigkeit der Bildung des Bromwasserstoffs aus seinen Elementen. Z. Phys. Chem. **57**, 168–175 (1906)
16. Smooke, M.D. (ed.): Reduced Kinetic Mechanisms and Asymptotic Approximations for Methane-Air Flames, vol. 384. Springer, Berlin (1991)
17. Keck, J.C., Gillespie, D.: Rate-controlled partial equilibrium method for treating reacting gas-mixtures. Combust. Flame **17**, 237–241 (1971)
18. Keck, J.C.: Rate-controlled constrained equilibrium theory of chemical reactions in complex systems. Prog. Energy Combust. Sci. **16**, 125–154 (1990)
19. Lam, S.H.: Using CSP to understand complex chemical kinetics. Combust. Sci. Technol. **89**, 375–404 (1993)
20. Lam, S.H., Goussis, D.A.: The CSP method of simplifying kinetics. Int. J. Chem. Kinet. **26**, 461–486 (1994)
21. Maas, U., Pope, S.B.: Simplifying chemical-kinetics: intrinsic low-dimensional manifolds in composition space. Combust. Flame **88**, 239–264 (1992)
22. Pope, S.B., Mass, U.: Simplifying chemical kinetics: trajectory-generated low-dimensional manifolds. FDA 93-11. Cornell University, Ithaca (1993)

23. Roussel, M.R., Fraser, S.J.: Global analysis of enzyme inhibition kinetics. *J. Phys. Chem.* **97**, 8316–8327 (1993)
24. van Oijen, J.A., de Goey, L.P.H.: Modelling of premixed laminar flames using flamelet-generated manifolds. *Combust. Sci. Technol.* **161**, 113–137 (2000)
25. Bongers, H., van Oijen, J.A., de Goey, L.P.H.: Intrinsic low-dimensional manifold method extended with diffusion. *Proc. Combust. Inst.* **29**, 1371–1378 (2002)
26. Gorban, A.N., Karlin, I.V.: Method of invariant manifold for chemical kinetics. *Chem. Eng. Sci.* **58**, 4751–4768 (2003)
27. Singh, S., Powers, J.M., Paolucci, S.: On slow manifolds of chemically reactive systems. *J. Chem. Phys.* **117**, 1482–1496 (2002)
28. Gear, C.W., Kaper, T.J., Kevrekidis, I.G., Zagaris, A.: Projecting to a slow manifold: singularly perturbed systems and legacy codes. *SIAM J. Appl. Dyn. Syst.* **4**, 711–732 (2005)
29. Bykov, V., Maas, U.: The extension of the ILDM concept to reaction-diffusion manifolds. *Combust. Theory Model.* **11**, 839–862 (2007)
30. Ren, Z., Pope, S.B., Vladimirovsky, A., Guckenheimer, J.M.: The invariant constrained equilibrium edge preimage curve method for the dimension reduction of chemical kinetics. *J. Chem. Phys.* **124**, Art. No. 114111 (2006)
31. Chen, J.-Y., Kollmann, W., Dibble, R.W.: PDF modelling of turbulent nonpremixed methane jet flames. *Combust. Sci. Technol.* **64**, 315–346 (1989)
32. Turányi, T.: Parameterization of reaction mechanisms using orthogonal polynomials. *Comput. Chem.* **18**, 45–54 (1994)
33. Christo, F.C., Masri, A.R., Nebot, E.M.: An integrated PDF/neural network approach for simulating turbulent reacting systems. *Proc. Combust. Inst.* **26**, 43–48 (1996)
34. Pope, S.B.: Computationally efficient implementation of combustion chemistry using *in situ* adaptive tabulation. *Combust. Theory Model.* **1**, 41–63 (1997)
35. Tonse, S.R., Moriarty, N.W., Brown, N.J., Frenklach, M.: PRISM: Piecewise Reusable Implementation of Solution Mapping. An economical strategy for chemical kinetics. *Isr. J. Chem.* **39**, 97–106 (1999)
36. Yang, B., Pope, S.B.: An investigation of the accuracy of manifold methods and splitting schemes in the computational implementation of combustion chemistry. *Combust. Flame* **112**, 16–32 (1998)
37. Xu, J., Pope, S.B.: PDF calculations of turbulent nonpremixed flames with local extinction. *Combust. Flame* **123**, 281–307 (2000)
38. Tang, Q., Xu, J., Pope, S.B.: PDF calculations of local extinction and NO production in piloted-jet turbulent methane/air flames. *Proc. Combust. Inst.* **28**, 133–139 (2000)
39. Lu, L., Ren, Z., Raman, V., Pope, S.B., Pitsch, H.: LES/FDF/ISAT computations of turbulent flames. In: Proceedings of CTR Summer Program 2004, Center For Turbulence Research, pp. 283–294, CTR, December 2004
40. Lu, L., Ren, Z., Lantz, S.R., Raman, V., Pope, S.B., Pitsch, H.: Investigation of strategies for the parallel implementation of ISAT in LES/FDF/ISAT computations. Paper presented at the 4th joint meeting of the U. S. Sections of the Combustion Institute, Philadelphia, PA, 21–23 March 2005
41. Singer, M.A., Pope, S.B.: Exploiting ISAT to solve the reaction-diffusion equation. *Combust. Theory Model.* **8**, 361–383 (2004)
42. Singer, M.A., Pope, S.B., Najm, H.N.: Operator-splitting with ISAT to model reacting flow with detailed chemistry. *Combust. Theory Model.* **10**, 199–217 (2006)
43. Gordon, R.L., Masri, A.R., Pope, S.B., Goldin, G.M.: A numerical study of auto-ignition in turbulent lifted flames issuing into a vitiated co-flow. *Combust. Theory Model.* **11**, 351–376 (2007)
44. Gordon, R.L., Masri, A.R., Pope, S.B., Goldin, G.M.: Transport budgets in turbulent lifted flames of methane autoigniting in a vitiated co-flow. *Combust. Flame* **151**, 495–511 (2007)
45. Schwer, D.A., Lu, P., Green, W.H. Jr.: An adaptive chemistry approach to modeling complex kinetics in reacting flows. *Combust. Flame* **133**, 451–465 (2003)
46. Ren, Z., Pope, S.B.: Species reconstruction using pre-image curves. *Proc. Combust. Inst.* **30**, 1293–1300 (2005)
47. Ren, Z., Pope, S.B., Vladimirovsky, A., Guckenheimer, J.M.: Application of the ICE-PIC method for the dimension reduction of chemical kinetics coupled with transport. *Proc. Combust. Inst.* **31**, 473–481 (2007)
48. Ren, Z., Pope, S.B.: Reduced description of complex dynamics in reactive systems. *J. Phys. Chem. A* **111**, 8464–8474 (2007).

49. Strang, G.: On the construction and comparison of difference schemes. *SIAM J. Numer. Anal.* **5**, 506–517 (1968)
50. Ren, Z., Pope, S.B.: Second-order splitting schemes for a class of reactive systems. *J. Comput. Phys.* (2008, submitted)
51. Davis, M.J., Skodje, R.T.: Geometric investigation of low-dimensional manifolds in systems approaching equilibrium. *J. Chem. Phys.* **111**, 859–874 (1999)
52. Ren, Z., Pope, S.B.: The use of slow manifolds in reactive flows. *Combust. Flame* **147**, 243–261 (2006)
53. Kaper, H.G., Kaper, T.J.: Asymptotic analysis of two reduction methods for systems of chemical reactions. *Physica D* **165**, 66–93 (2002)
54. Goussis, D.A., Valorani, M., Creta, F., Najm, H.N.: Reactive and reactive-diffusive time scales in stiff reaction-diffusion systems. *Prog. Comput. Fluid Dyn.* **5**, 316–326 (2005)
55. Yannacopoulos, A.N., Tomlin, A.S., Brindley, J., Merkin, J.H., Pilling, M.J.: The use of algebraic sets in the approximation of inertial manifolds and lumping in chemical kinetic systems. *Physica D* **83**, 421–449 (1995)
56. Maas, U., Pope, S.B.: Implementation of simplified chemical kinetics based on intrinsic low-dimensional manifolds. *Proc. Combust. Inst.* **24**, 103–112 (1992)
57. Pope, S.B.: Accessed compositions in turbulent reactive flows. *Flow Turbul. Combust.* **72**, 219–243 (2004)
58. Lam, S.H.: Reduced chemistry-diffusion coupling. *Combust. Sci. Tech.* **179**, 767–786 (2007)
59. Ren, Z., Pope, S.B.: Transport-chemistry coupling in the reduced description of reactive flows. *Combust. Theory Model.* **11**, 715–739 (2007)